HHS Public Access

Author manuscript

Int J Cancer. Author manuscript; available in PMC 2020 October 15.

Published in final edited form as:

Int J Cancer. 2019 October 15; 145(8): 2122–2134. doi:10.1002/ijc.32155.

DNMT3a-triggered downregulation of $K_{2p}1.1$ gene in primary sensory neurons contributes to paclitaxel-induced neuropathic pain

Qingxiang Mao[1,2], **Shaogen Wu**[1], **Xiyao Gu**[1], **Shibin Du**[1], **Kai Mo**[1], **Linlin Sun**[1], **Jing Cao**[1,3], **Alex Bekker**[1], **Liyong Chen**[2], **Yuan-Xiang Tao**[1]

[1]Department of Anesthesiology, New Jersey Medical School, Rutgers, The State University of New Jersey, Newark, NJ 07103, USA

[2]Department of Anesthesiology, Daping Hospital, Institute of Surgery Research, Third Military Medical University (Army Medical University), Chongqing 400042, China

[3]Neuroscience Research Institute, Zhengzhou University Academy of Medical Sciences, Zhengzhou, Henan 45001, China

Abstract

Antineoplastic drugs induce dramatic transcriptional changes in dorsal root ganglion (DRG) neurons, which may contribute to chemotherapy-induced neuropathic pain. $K_{2p}1.1$ controls neuronal excitability by setting the resting membrane potential. Here, we report that systemic injection of the chemotherapy agent paclitaxel time-dependently downregulates the expression of *$K_{2p}1.1$* mRNA and its coding $K_{2p}1.1$ protein in the DRG neurons. Rescuing this downregulation mitigates the development and maintenance of paclitaxel-induced mechanical allodynia and heat hyperalgesia. Conversely, in the absence of paclitaxel administration, mimicking this downregulation decreases outward potassium current and increases excitability in the DRG neurons, leading to the enhanced responses to mechanical and heat stimuli. Mechanically, the downregulation of DRG *$K_{2p}1.1$* mRNA is attributed to paclitaxel-induced increase in DRG DNMT3a, as blocking this increase reverses the paclitaxel-induced the decrease of DRG $K_{2p}1.1$ and mimicking this increase reduces DRG $K_{2p}1.1$ expression. In addition, paclitaxel injection increases the binding of DNMT3a to the *$K_{2p}1.1$* gene promoter region and elevates the level of DNA methylation within this region in the DRG. These findings suggest that DNMT3a-triggered downregulation of DRG $K_{2p}1.1$ may contribute to chemotherapy-induced neuropathic pain.

Corresponding authors: Dr. Yuan-Xiang Tao, Department of Anesthesiology, New Jersey Medical School, Rutgers, The State University of New Jersey, 185 S. Orange Ave., MSB, E-661, Newark, NJ 07103. Tel: +1-973-972-9812; Fax: +1-973-972-1644. yuanxiang.tao@njms.rutgers.edu, Liyong Chen, Department of Anesthesiology, Daping Hospital, Institute of Surgery Research, The Third Military Medical University (Army Medical University), 10 Changjiang Zhilu, Yuzhong District, Chongqing, China, 400042. Tel: +8602368757081, Fax: +862368757087. mzkcly@aliyun.com.

Author contributions

Y.X.T. and L.C. conceived the project and supervised all experiments. Q.M., S.W., and Y.X.T. assisted with experimental design. Q.M., S.W., K.M., L.S., J.C. and X.G. carried out animal surgery, behavioral test, and molecular, biochemical and electrophysiological experiments. Q.M., S.W., X.G., A.B., L.C., and Y.X.T. analyzed the data. Q.M. and Y.X.T. drafted the manuscript. All authors read and discussed the final manuscript.

Conflict of interests

The authors declare that they have no conflict of interest.

Keywords

$K_{2p}1.1$; DNMT3a; dorsal root ganglion; paclitaxel; neuropathic pain

Introduction

Among the distressing symptoms of cancer patients receiving chemotherapy, the most common are sensory dysfunction and pain [1, 2], which are typically symmetrical in a socking-glove distribution [3, 4]. The incidence and severity of these symptoms are correlated with duration and dose of chemotherapy drugs [5, 6]. Thus, nearly all patients eventually discontinue cancer therapy and have the reduced survival rates.

Despite recent progress, the mechanism of chemotherapy-induced peripheral neuropathic pain (CIPNP) is still elusive. Chemotherapy drugs poorly penetrate into the central nervous system [7, 8], but they have unrestricted access to dorsal root ganglion (DRG) due to the lack of an effective vascular permeability barrier [9, 10]. Chemotherapeutic paclitaxel produced ectopic spontaneous activity in DRG neuronal somata [11–14]. This abnormal activity, which has been identified as a CIPNP contributor [11–14], may be related to the changes in the gene expression at the transcriptional and translational levels in the DRG after chemotherapy drug treatments [11–20]. Understanding how chemotherapy drugs drive these changes is essential for improving patient care.

The two-pore domain background potassium (K_2P) channel family and the leak currents carried by K_2P channels are key determinants of neuronal activity throughout the nervous system, as disrupting this leak currents can result in depolarization and increased neuronal excitability [21]. $K_{2p}1.1$, the first identified mammalian K_2P channel, is highly expressed in DRG neurons [22, 23]. Peripheral nerve injury leads to a marked downregulation of $K_{2p}1.1$ in the injured DRG [22, 23]. Rescuing this downregulation attenuated spinal nerve ligation-induced pain hypersensitivities [22]. However, the mechanisms underlying peripheral nerve injury-induced DRG $K_{2p}1.1$ downregulation are still elusive. More importantly, whether and how DRG $K_{2P}1.1$ participates in the CIPNP genesis is unknown, given that the underlying mechanism may vary with different neuropathic pain etiology.

We report here that $K_{2P}1.1$ mRNA and protein are significantly and time-dependently decreased in the DRG after paclitaxel injection. This decrease is attributed to the paclitaxel-induced upregulation of *de novo* methyltransferase DNMT3a in the DRG. Rescuing DRG $K_{2P}1.1$ downregulation mitigates the development and maintenance of paclitaxel-induced mechanical and thermal pain hypersensitivities. $K_{2P}1.1$ is likely a potential target in the management of CIPNP.

Materials and methods

Animal preparation

Adult male mice (8–10 weeks) were used for the experiments. The CD1 mice were purchased from Charles River Laboratories (Wilington). *Dnmt3a*$^{fl/fl}$ mice were provided by Dr. Eric J Nestler. Male sensory-specific Advillin-Cre$^{+/-}$ mice were crossed with female

Dnmt3a$^{fl/fl}$ mice to obtain *Dnmt3a* conditional knockout (*Dnmt3a* KO) mice. All procedures used were approved by the Animal Care and Use Committee at the Rutgers New Jersey Medical School and consistent with the ethical guidelines of the US NIH and the IASP. The group sizes were based on previous reports [24, 25].

DRG microinjection

In brief, a dorsal midline incision was made in the lower lumbar region, and the left L3–4 articular processes were exposed. After the lamina was removed, the L3–4 DRGs were exposed. The siRNA (1 μl/DRG, 40 μM) or viral solution (1 μl/DRG, 10^{12} particles/ml) was injected into the left L3 and L4 DRGs with a glass micropipette [24, 25]. TurboFect *in vivo* transfection reagent (Thermo Scientific Inc.) was used as a delivery vehicle [26–28].

Paclitaxel-induced neuropathic pain model

Briefly, paclitaxel (4 mg/kg; dissolved in the vehicle) or vehicle (a mixture of ethanol and Cremophor EL(1:1)) was injected intraperitoneally (i.p.) every other day for 4 consecutive days [29].

Behavioral testing

Mechanical and heat testing, conditioned place preference (CPP) were performed as previously described [24, 25, 30, 31].

For mechanical testing, two different von Frey filaments (0.17 and 0.4 g) were applied the plantar surface of both hind paws. Each stimulation was repeated 10 times. The occurrence of paw withdrawal was expressed as a paw withdrawal frequency.

Paw withdrawal latency (PWL) to noxious heat was measured using the Model 336 Analgesia Meter. A beam of light that provided radiant heat was aimed at the middle of the plantar surface of each hind paw. The time from turning on the light beam to the foot lift was defined as paw withdrawal latency.

In the CPP test, the preconditioning was first carried out 30 min daily for 3 days (MED Associates Inc.). On the 4th day, length of time spent in each chamber was recorded for 15 min (900 sec). The conditioning protocol was carried out on days 5, 6 and 7 with the internal door closed. Mice were intrathecally injected with saline (5 μl) and paired with one conditioning chamber in the morning, following by intrathecally injection with 5 μl lidocaine (0.4 %) later in the afternoon and paired with other conditioning chamber, or *vice versa*. On day 8, the mice were placed in one chamber with free access to both chambers and the duration spent in each chamber was recorded for 15 min.

Plasmid construction and siRNA or virus preparation

According to our previously published protocols [25], full-length mouse $K_{2p}1.1$ cDNA was synthesized and amplified from total RNA of mouse DRG. The cDNA was inserted into the pro-viral plasmid. AAV-DJ viral particles carrying the $K_{2p}1.1$ cDNA were produced as described previously [22]. AAV5-GFP and AAV5-Cre were purchased from UNC Vector Core. HSV-GFP and HSV-*Dnmt3a* were provided by Dr. Eric J Nestler (Icahn School of Medicine

at Mount Sinai). *$K_{2p}1.1$* siRNA (catalog#: s68672) and its negative control siRNA (catalog#: 4457287) were purchased from Ambion of Life Technologies (Carlsbad).

DRG neuron culture and transfection—DRGs of 3-week-old mice were collected and treated with enzyme solution at 37°C for 20 minutes. After centrifugation, dissociated cells were resuspended in DH10 and incubated in a six-well plate. One day later, 1μl of virus (titer ≥1×10^{12}/ml) or 100 ng siRNA with Lipofectamine 2000 (Invitrogen) was added into the medium. Three days after transduction/transfection, the cells were collected for RT-PCR or Western blot analysis.

Total RNA preparation and quantitative real-time RT-PCR

Briefly, bilateral L4/5 mice DRGs were rapidly collected and subjected to total RNA extraction kit (Qiagen) [30, 31]. RNA was then reverse-transcribed using the ThermoScript reverse transcriptase (Invitrogen) and oligo (dT) primers. Each cDNA was run in triplicate in a 20 μl reaction with forward and reverse primers (Supplementary Table 1) and SYBR Green Supermix (Bio-Rad). All real time PCR reactions were performed with an initial 3 min incubation at 95 °C, followed by 40 cycles at 95 °C for 10 s, 60 °C for 30 s, and 72 °C for 30 s. Ratios of mRNA levels were calculated by using the ΔCt method ($2^{-\Delta\Delta Ct}$). All data were normalized to internal control *Gapdh*.

Western blot analysis

As previously described [30, 31], bilateral lumber mice DRGs were collected. DRG tissues were homogenized and centrifugalized at 4 °C. The supernatant was collected, and the pellet (nuclei and debris fraction) was dissolved in lysis buffer and then sonicated on ice. The membrane or nuclei samples were heated at 99°C for 5 min, loaded and run onto precast polyacrylamide gel (Bio-Rad), then were electrophoretically transferred onto nitrocellulose membranes. After blocking, The membranes were incubated with primary rabbit anti-$K_{2p}1.1$ (1:1,000, Alomone), mouse anti-$K_v1.2$ (1:500, NeuroMab), rabbit anti-GAPDH (1:2,000, Santa Cruz Biotechnology), rabbit anti-DNMT3a (1:500, Cell Signaling Technology), rabbit anti-DNMT3b (1:500, Santa Cruz Biotechnology), rabbit anti-DNMT1 (1:1,000, Cell Signaling Technology), or rabbit anti-H3 (1:2,000, Cell Signaling Technology) at 4 °C overnight. After secondary antibody incubation, the blots were developed with chemiluminescent regents. The intensities of blots were quantified with Image Lab software.

Immunohistochemistry

As described previously [30, 31], after mice were perfused with PBS followed by fixation with 4% paraformaldehyde, L3/4 DRGs were removed, post-fixed and dehydrated overnight at 4°C. For single labeling, 20 μm sections were incubated alone with primary rabbit anti-$K_{2p}1.1$ (1:1,000) over two nights at 4°C after being blocked. The sections were then washed with PBS and incubated with goat anti-rabbit IgG conjugated with Cy2 for 2 h at room temperature. For double labeling, the sections were incubated with primary rabbit anti-$K_{2p}1.1$ plus mouse anti-DNMT3a (1:500, Abcam). The sections were washed and re-incubated with a mixture of goat anti-rabbit IgG conjugated with Cy2 and donkey anti-mouse IgG conjugated with Cy3 for 2 h at room temperature.

Chromatin immunoprecipitation (ChIP) assay

The ChIP assays were conducted using the EZ-Magna ChIP™ G - Chromatin Immunoprecipitation Kit (EMD Millipore) [25]. Briefly, the homogenate from the DRG was cross-linked with 1% formaldehyde and terminated by glycine. After centrifugation, the collected pellet was resuspended with nuclear lysis buffer and sonicated to shear the cross-linked DNA. After centrifugation, the supernatant was diluted and respectively subjected to immunoprecipitation overnight at 4°C with protein G magnetic beads plus 3 μg of rabbit anti-DNMT3a (Abcam) or 3 μg of normal rabbit serum. Input was used as a positive control. After incubation, protein G magnetic beads were pelleted with the magnetic separator and washed respectively with low salt buffer, high salt buffer, LiCl buffer and TE buffer. The protein/DNA complexes were eluted and reversed to free DNA. The DNA fragments were purified and identified using PCR/real-time PCR with the primers (Supplementary Table 1).

Methylated DNA immunoprecipitation (MeDIP)

Genomic DNA was extracted and purified from the DRG tissue using DNeasy Blood & Tissue Kit (Qiagen). The purified DNA was sheared with dsDNA Shearase Plus (Zymo Research) into 100–500 bp fragments [32]. The fragments of DNA were purified using DNA Clean & Concentrator kit (Zymo Research), then were denatured and subjected to immunoprecipitation at 37°C for 1 h with ZymoMag Protein A beads plus 1.6 μl mouse anti-5-methylcytosine antibodies (Zymo Research) [33]. After incubation, the beads were pelleted with the magnetic separator and washed respectively with MIP buffer and DNA elution buffer. The recovered DNA was collected in the supernatant and was identified using PCR/real-time PCR with the primers.

Whole-cell patch clamp recording

As described previously [25, 30], the freshly dissociated L3/4 DRG neurons from the mice were prepared. The electrode resistances of micropipettes ranged from 3 to 5 MΩ. Neurons were voltage-clamped with an Axon 700B amplifier. The intracellular pipette solution contained (in mM) 120 CsF, 20 KCl, 2 $MgCl_2$, 10 EGTA, 4 MgATP, 10 HEPES, and CsOH to adjust the pH to 7.2. The extracellular solution composed of (in mM) 5 KCl, 30 TEA-Cl, 120 Choline chloride, 1 $MgCl_2$, 2 $CaCl_2$, 1 $CdCl_2$, 10 HEPES, 10 D-glucose and TEA-OH to adjust the pH to 7.4. TEA was used to block the voltage-gated potassium channel and Cs to block the inward rectifier potassium channel.

To record the action potential and spontaneous activity, we switched the recording mode into current clamp. Neurons were placed in a chamber with the temperature controlled at 37°C with TC-344C (Warner Instruments) and perfused with extracellular solution consisting of (in mM) 140 NaCl, 4 KCl, 2 $CaCl_2$, 2 $MgCl_2$, 10 HEPES and 5 glucose. The intracellular pipette solution contained (in mM) 135 KCl, 3 Mg-ATP, 0.5 Na_2ATP, 1.1 $CaCl_2$, 2 EGTA and 5 glucose. The spontaneous activity was recorded in gap-free protocol for 5min. The resting membrane potential was recorded 3–5 min after a stable recording was first achieved. Depolarizing currents of 100–1400pA (200 ms duration) were delivered in increments of 100 pA until an action potential (AP) was evoked. The injection current threshold was defined as the minimum current required to evoke the first AP. The AP threshold was

defined as the first point on the rapid rising phase of the spike at which the change in voltage exceeded 50 mV/ms. The AP amplitude was measured between the peak and the baseline.

Statistical analysis

All of the results are given as the mean ± S.E.M. The data were statistically analyzed with two-tailed, paired Student's *t*-test and a one-way or two-way ANOVA. When ANOVA showed a significant difference, pairwise comparisons between means were tested by the *post hoc* Turkey method (SigmaPlot 12.5, San Jose, CA). Significance was set at $P < 0.05$.

Results

$K_{2p}1.1$ downregulation in the DRG after paclitaxel injection

Consistent with the previous reports [29, 34], systemic injection (i.p.) of paclitaxel, but not vehicle, produced long-lasting mechanical allodynia, as evidenced by the significant increases in paw withdrawal frequencies in the response to von Frey filament stimuli and heat hyperalgesia as demonstrated by the marked reductions in paw withdrawal latencies to heat stimulation on both sides (Fig. 1a-1c; Supplementary Fig. 1a-1c). These pain hypersensitivities started on day 7 after the first injection of paclitaxel and persisted for at least 21 days (Fig. 1a-1c; Supplementary Fig. 1a-1c). Paclitaxel injection also time-dependently reduced the amounts of *$K_{2p}1.1$* mRNA and protein in the DRG. The levels of *$K_{2p}1.1$* mRNA in both lumbar 3 and 4 (L3/4) DRGs were decreased by 43.8%, 37.9% and 43.1% on days 7, 14 and 21, respectively, following first injection of paclitaxel as compared to naive mice (0 day. Fig. 1d). Consistently, the amounts of $K_{2p}1.1$ protein in both L3/4 DRGs were reduced by 41.4%, 53.8% and 44.2% on days 7, 14 and 21 respectively, as compared to naive mice (Fig. 1e). As expected, vehicle injection did not produce any changes in basal levels of *$K_{2p}1.1$* mRNA and protein in the DRGs on either side (Fig. 1d and 1e). Injection of neither paclitaxel nor vehicle led to changes in basal amounts of $K_v1.2$, MOR, and KOR proteins in the DRG during the observation period (Supplementary Fig. 1d and 1e). Injection of paclitaxel, but not vehicle, decreased the number of $K_{2p}1.1$-labelled neurons by 59.2% in the left L4 DRG on day 14 from the paclitaxel-injected mice compared to those from the vehicle-injected mice (Fig. 1f). No significant expressional change in $K_{2p}1.1$ protein was found in the L3/4 spinal cord after paclitaxel injection (Supplementary Fig. 1f).

Overexpressing $K_{2p}1.1$ in unilateral DRG blunted paclitaxel-induced neuropathic pain on the ipsilateral side

We first examined whether the reduced *$K_{2p}1.1$* expression in the DRG contributed to the development of paclitaxel-induced pain hypersensitivity. To this end, we constructed AAV-DJ virus expressing full-length *$K_{2p}1.1$* mRNA (AAV-$K_{2p}1.1$) and pre-microinjected this virus into unilateral L3/4 DRGs to rescue paclitaxel-induced downregulation of $K_{2p}1.1$. AAV-DJ expressing enhanced GFP (AAV-GFP) was used as a control. Given that AAV-DJ requires 3–4 weeks to become expressed [22], paclitaxel or vehicle was injected intraperitoneally 4 weeks after viral microinjection. Mechanical allodynia and heat hyperalgesia were observed on both sides of the AAV-GFP plus paclitaxel-treated group from day 7 to 14 after first injection of paclitaxel (Fig. 2a-2c; Supplementary Fig. 2a-2c). In

contrast, these pain hypersensitivities were abolished on the ipsilateral side, but not the contralateral side, of the AAV-K_{2p}1.1 plus paclitaxel-treated group (Fig. 2a-2c; Supplementary Fig. 2a-2c). Compared to baseline levels, there were no significant increases in paw withdrawal frequencies in response to von Frey filament stimuli and no marked decrease in paw withdrawal latency to heat stimulation on the ipsilateral side of the AAV-K_{2p}1.1 plus paclitaxel-treated group (Fig. 2a-2c). As expected, microinjection of neither AAV-K_{2p}1.1 nor AAV-GFP altered basal paw withdrawal responses on both groups (Fig. 2a-2c; Supplementary Fig. 2a-2c). As shown in Supplementary Table 2, mice from the four treated groups displayed normal locomotor functions including placing, grasping and righting reflexes.

On day 14 after first injection of paclitaxel, the injected L3/4 DRGs were collected to examine the level of K_{2p}1.1 in these DRGs from the treated groups. The amount of K_{2p}1.1 protein was markedly reduced in the injected DRGs from the AAV-GFP plus paclitaxel-treated group compared to the naive group (Fig. 2d). This reduction was completely rescued in the AAV-K_{2p}1.1 plus paclitaxel-treated group (Fig. 2d). In the AAV-K_{2p}1.1 plus vehicle-treated group, the level of K_{2p}1.1 protein in the injected DRG significantly increased by 3.6-fold compared to the naïve group (Fig. 2d).

We also examined whether rescuing DRG K_{2p}1.1 downregulation reversed the existing pain hypersensitivity. Two weeks after viral microinjection into unilateral L3/4 DRGs, mice received i.p. injection of paclitaxel. Mechanical allodynia and heat hyperalgesia were completely developed on both sides of the paclitaxel plus AAV-GFP- or AAV-K_{2p}1.1-treated groups 7 days after first injection of paclitaxel (Fig. 2e-2g; Supplementary Fig. 2d-2f). These pain hypersensitivities were markedly blocked on ipsilateral hindpaws of the AAV-K_{2p}1.1 plus paclitaxel-treated mice, but not on that of the AAV-GFP plus paclitaxel-treated mice on days 14 and 21 (Fig. 2e-2g). Mechanical allodynia and heat hyperalgesia were not affected on the contralateral side of both groups (Supplementary Fig. 2d-2f).

DRG K_{2p}1.1 downregulation leads to pain hypersensitivity

Next, we determined whether mimicking paclitaxel-caused downregulation of DRG K_{2p}1.1 altered the nociceptive threshold. We carried out *K_{2p}1.1*-specfic short interfering RNA (K_{2p}1.1-siRNA) to knock down K_{2p}1.1. *K_{2p}1.1* negative control siRNA (NC-siRNA) was used as a control. We first checked the inhibitory efficiency and specificity of K_{2p}1.1-siRNA in mouse cultured DRG neurons and found that K_{2p}1.1-siRNA significantly reduced the mRNA and protein levels of K_{2p}1.1 (Fig. 3a and 3b). Neither K_{2p}1.1-siRNA nor NC-siRNA altered the expressions of other potassium channel mRNAs, including *KCNK6, Kcna1, Kcna2, and Kcna4* mRNAs and K_v1.2 protein (Fig. 3a and 3b). We then microinjected K_{2p}1.1-siRNA or NC-siRNA into the unilateral L3/4 DRGs of naïve mice. Compared with naive mice, the level of K_{2p}1.1 protein was significantly decreased by 64.4% in the K_{2p}1.1-siRNA-treated DRGs on day 5 (Fig. 3c). As expected, DRG K_{2p}1.1-siRNA microinjection did not alter the *in vivo* expression of other potassium channels, like K_v1.2 protein, in the injected DRGs (Fig. 3c). There were no marked changes of basal expression of K_{2p}1.1 or K_v1.2 in the NC-siRNA-treated DRGs when compared to naive mice (Fig. 3c).

The mice injected with K_{2p}1.1-siRNA (not NC-siRNA) displayed significant increases in response to von Frey filament stimuli and decrease in response to heat stimulation on days 3, 5, and 7 on the ipsilateral side (Fig. 3d-3f). Neither K_{2p}1.1-siRNA nor NC-siRNA affected locomotor functions (Supplementary Table 2) or the basal paw withdrawal responses on the contralateral side (Supplementary Fig. 3a-3c). These behavioral observations indicate that the reduced K_{2p}1.1 in the DRG produces mechanical allodynia and heat hyperalgesia, major clinical symptoms of paclitaxel-induced neuropathic pain, in the absence of paclitaxel injection.

K_{2p}1.1 knockdown reduces outward potassium channel current and increases excitability and in DRG neurons

We further examined whether mimicking paclitaxel-caused downregulation of DRG K_{2p}1.1 affected DRG neuronal excitability. Using whole cell patch clamp recording, we first recorded the outward potassium channel current in the injected L3/4 DRGs from day 3 to day 7 post-microinjection of NC-siRNA or K_{2p}1.1-siRNA. Under the conditions of voltage gated potassium channel and inward rectifying potassium channel blockage, compared to the NC-siRNA-treated group, the outward potassium current was significantly reduced in large, medium and small DRG neurons from the K_{2p}1.1-siRNA-treated group (Fig. 4a-4c, Supplementary Fig. 4a-4f). To confirm whether these reductions were caused by K_{2p}1.1 knockdown, we applied 0.5 mM quinine, an effective K_{2p}1.1 channel inhibitor, in bath. After quinine treatment, the reductions in the outward potassium currents in large, medium and small DRG neurons from the NC-siRNA-treated group were much greater than those from the K_{2p}1.1-siRNA-treated group (Fig. 4a-4c, Supplementary Fig. 4a-4f). When tested at +40 mV, the differences in quinine-sensitive outward potassium current densities in large, medium and small DRG neurons were 48.7, 9.9 and 15.8 pA/pf, respectively, between the two groups (Fig. 4c, Supplementary Fig. 4c, 4f).

We then used whole cell current clamp recording to examine neuronal excitability in the injected L3/4 DRGs from day 3 to day 7 post-microinjection of NC-siRNA or K_{2p}1.1-siRNA. Compared to the NC-siRNA-treated group, the large, medium and small neurons in the K_{2p}1.1-siRNA-treated mice exhibited increases by 10.6, 8.6 and 7.9 mV, respectively, in the resting membrane potentials (Fig. 4d), and decreases by 568, 183 and 179 pA, respectively, in the current thresholds (Fig. 4e). Furthermore, K_{2p}1.1-siRNA microinjection markedly increased the numbers of action potentials in large, medium and small DRG neurons evoked by stimulation of ≥ 300, 500, and 100 pA, respectively, (Fig. 4f-4g), although this microinjection did not alter the membrane input resistance or other action potential parameters, such as amplitude, threshold, overshoot and after-hyperpolarization amplitude (Supplementary Table 3). Compared to the NC-siRNA-treated group, the percentage numbers of spontaneous activity neurons significantly increased by 24%, 36% and 38% and the frequencies of spontaneous activity markedly elevated by 1.67, 1.95 and 3.26 Hz, respectively, in the large, medium and small neurons from the K_{2p}1.1-siRNA-treated group (Fig. 4h-4j). The evidence indicates that DRG microinjection of K_{2p}1.1 siRNA increased DRG neuronal excitability.

Increased DNMT3a in DRG is required for paclitaxel-induced neuropathic pain

How was DRG *$K_{2p}1.1$* mRNA downregulated after systemic injection of paclitaxel? Given that DNA methylation silences gene expression [35], we assumed that DNA methylation may be involved in paclitaxel-induced downregulation of *$K_{2p}1.1$* mRNA in DRG. We first examined the expression of three DNA methyltransferases (DNMT1, DNMT3a and DNMT3b) and three DNA demethylation enzymes (TET1, TET2 and TET3) [35] in DRG after paclitaxel injection. Interestingly, paclitaxel injection time-dependently increased the expression of DNMT3a, but not DNMT1, DNMT3b, TET1, TET2 or TET3 (Fig. 5a; Supplementary Fig. 5a). The level of DNMT3a was increased by 3.1-fold on day 7, 2.3-fold on day 14 and 1.0-fold on day 21 after first injection of paclitaxel as compared to naive mice (Fig. 5a). In the spinal cord, the expression of neither three DNA methyltransferases nor three DNA demethylation enzymes were altered (Supplementary Fig. 5b-5c).

We then observed whether the increased DNMT3a in the DRG contributed to pain hypersensitivities after paclitaxel injection. Effect of i.p. co-administration of RG108 (0.4 mg/kg, once a day for 7 days), a specific DNMT inhibitor [36], on paclitaxel-induced pain hypersensitivity was examined. Compared to the paclitaxel plus vehicle-treated group, RG108 significantly blocked the paclitaxel-induced mechanical allodynia (Fig. 5b and 5c; Supplementary Fig. 6a and 6b) and heat hyperalgesia (Fig. 5d; Supplementary Fig. 6c) on days 7, 14, and 21 after the first injection of paclitaxel on both sides. As expected, i.p. injection of RG108 alone did not alter basal paw withdrawal responses on either side in the RG108 plus vehicle-treated group (Fig. 5b-5d; Supplementary Fig. 6a-6c). I.p. injection of RG108 (0.4 mg/kg, daily for 6 days) starting at day 7 after the first injection of paclitaxel also ameliorated the paclitaxel-induced mechanical allodynia and heat hyperalgesia on days 11 and 13 after the first injection of paclitaxel on both sides (Supplementary Fig. 7). Moreover, on day 14 after the first injection of paclitaxel, i.p. administration of RG108 attenuated the paclitaxel-induced and stimulation-independent spontaneous ongoing pain, as evidenced by no marked preference for either the saline- or lidocaine-paired chamber in the RG108 plus paclitaxel-treated group. This was in contrast to the paclitaxel-induced spontaneous ongoing pain as indicated by the obvious preference (that is, spending more time) for the lidocaine-paired chamber in the vehicle plus paclitaxel-treated group (Fig. 5e-5f).

Due to the potential limitation of i.p. administration of RG108 in anatomical and biochemical specificity, we further confirm the role of DRG increased DNMT3a in paclitaxel-induced pain hypersensitivities through carrying out conditional *Dnmt3a* KO mice. Compared to the *Dnmt3a*$^{fl/fl}$ mice, the *Dnmt3a* KO mice failed to produce mechanical allodynia or heat hyperalgesia on both sides on days 7, 14, and 21 after the first injection of paclitaxel (Fig. 5g-5i; Supplementary Fig. 8a-8c).

Increased DNMT3a contributes to paclitaxel-induced downregulation of $K_{2p}1.1$ in DRG neurons

Finally, we explored whether the increased DNMT3a was involved in paclitaxel-induced downregulation of $K_{2p}1.1$ in the DRG. DRG overexpression of DNMT3a through microinjection of herpes simplex virus (HSV) that expresses full-length *Dnmt3a* (HSV-

DNMT3a) into the unilateral L3/4 DRGs dramatically decreased the level of $K_{2p}1.1$ protein as compared to naive mice on day 5 post-microinjection (Fig. 6a). As a control, microinjection of HSV-GFP did not alter basal level of $K_{2p}1.1$ protein expression in the injected DRG (Fig. 6a). In contrast, the basal amount of $K_{2p}1.1$ protein significantly increased in the DRG of conditional DNMT3a KO mice (Fig. 6b). Consistent with the observations above, i.p. injection of paclitaxel upregulated DNMT3a expression and downregulated $K_{2p}1.1$ expression in the DRGs of the $DNMT3a^{fl/fl}$ mice on day 7 post-injection (Fig. 6b). These changes were not seen in the DRGs of the conditional DNMT3a KO mice (Fig. 6b). Because approximately 85.1% (468/550) of $K_{2p}1.1$-labelled neurons co-expressed with DNMT3a in DRG (Fig. 6c), it is very likely that $K_{2p}1.1$ expression was regulated directly by DNMT3a in DRG neurons. In line with this conclusion, overexpression of DNMT3a, through transduction of HSV-DNMT3a in cultured DRG neurons of $DNMT3a^{fl/fl}$ mice, decreased the levels of *$K_{2p}1.1$* mRNA and protein (Supplementary Fig. 9a-9b), whereas knockdown of DNMT3a through transduction of AAV5-Cre in the cultured DRG neurons of $DNMT3a^{fl/fl}$ mice substantially increased the level of $K_{2p}1.1$ protein (Supplementary Fig. 9b). This increase could be blocked by co-transduction of AAV5-Cre and HSV-DNMT3a (Supplementary Fig. 9b). The findings indicate that DNMT3a participates in paclitaxel-induced $K_{2p}1.1$ downregulation in the DRG.

We further carried out ChIP assay and reported that DNMT3a interacted with a region (−596/−406 bp) of the *$K_{2p}1.1$* gene promoter, as evidenced by the amplification of only this region (out of 8 regions from –791 to +661 bp) from the complexes immunoprecipitated with DNMT3a antibody in nuclear fractions from the DRGs of naïve mice (Fig. 6d). The binding activities of DNMT3a to this region in the DRGs on day 14 after first injection of paclitaxel increased by 3.2-fold, compared to the vehicle group (Fig. 6e). This increased binding activity might alter the DNA methylation pattern and level within the DNMT3a-binding sites following paclitaxel injection. Indeed, we used the anti-5-mC-mediated MeDIP assay and showed that the level of DNA methylation within the region (−596/−406 bp) of the *$K_{2p}1.1$* gene promoter increased significantly in the DRGs of the $Dnmt3a^{fl/fl}$ mice on day 14 after paclitaxel injection as compared to the vehicle group (Fig. 6f). This increase was DNMT3a-dependent, as the conditional DNMT3a KO mice failed to display the paclitaxel-induced increases in DNA methylation level in the DRGs (Fig. 6f). In addition, basal level of DNA methylation within the region (−596/−406 bp) of the *$K_{2p}1.1$* gene promoter markedly decreased in the DRGs from the vehicle-treated conditional DNMT3a KO mice, compared to the vehicle-treated $DNMT3a^{fl/fl}$ mice (Fig. 6f). The data suggest that DNMT3a-triggered DNA methylation at the range of −596 to −406 bp sites may involve in paclitaxel-induced downregulation of DRG $K_{2p}1.1$.

Discussion

Pain is a major symptom reported by the CIPNP patients. Current treatment for CIPNP has limited analgesic efficacy. Understanding the mechanisms that underlie this disorder may open a new avenue for CIPNP management. The present study demonstrated that systemic administration of paclitaxel led to a DNMT3a-triggered decrease in $K_{2p}1.1$ expression in DRG neurons. Rescuing this decrease alleviated the induction and maintenance of paclitaxel-induced mechanical allodynia and heat hyperalgesia. Mimicking this decrease

produced mechanical allodynia and heat hyperalgesia in the absence of paclitaxel treatment. Thus, DRG $K_{2p}1.1$ likely contributes to the mechanisms that underlie the CIPNP.

The expression of $K_{2p}1.1$ in the DRG can be regulated following peripheral noxious stimulation. I.p. injection of paclitaxel not only downregulated the expression of *$K_{2p}1.1$* mRNA and protein, but also reduced the number of $K_{2p}1.1$-positive neurons in the DRG. Similar downregulation was also seen in the ipsilateral DRG following complete Freund's adjuvant-induced peripheral inflammation, spared nerve injury, spinal nerve ligation, and axotomizing sciatic nerve [22, 37–39]. However, how these peripheral noxious stimuli downregulate *$K_{2p}1.1$* gene expression in the DRG neurons is still unclear. We showed that DRG *$K_{2p}1.1$* mRNA reduction may be associated with increased DNMT3a in the DRG under paclitaxel-induced conditions. DNMT3a is expressed exclusively in DRG neurons [25]. The majority of $K_{2p}1.1$-labelled DRG neurons co-express DNMT3a. Genetic knockout of DNMT3a in DRG avoided the downregulation of $K_{2p}1.1$ induced by paclitaxel, whereas mimicking paclitaxel-induced increase of DNMT3a via genetic overexpression reduced the DRG $K_{2p}1.1$ in naive mice. Our *in vitro* DRG neuronal cultured studies further verified direct regulation of DNMT3a on the expression of $K_{2p}1.1$. Our ChIP assay also revealed the direct binding of DNMT3a to the *$K_{2p}1.1$* gene promoter region (−596/−406 bp). Paclitaxel injection increased this binding activity and elevated the level of DNA methylation within this region. The latter is DNMT3a-dependent, as the paclitaxel-induced elevation in DNA methylation within this region was abolished in DRG of the conditional DNMT3a KO mice. Thus, DNMT3a-triggered DNA methylation within the *$K_{2p}1.1$* gene promoter participates in paclitaxel-induced downregulation in the DRG, likely through physically blocking the binding of some transcription factors and/or functioning as docking sites for some transcriptional repressors/corepressors [35, 40, 41]. It is worth mentioning that the expressional level of DNMT3a returned to basal level on day 21 post-injection, whereas, at this time point, paclitaxel injection still produced a significant decrease in DRG $K_{2p}1.1$ expression. Therefore, how $K_{2p}1.1$ is downregulated in the DRG at the late phase post-paclitaxel injection is still elusive. Given that the DNMT inhibitor RG108 systemically administered once daily for 7 days had marked effects on pain hypersensitivities on day 21 post-paclitaxel injection, it is very likely that the increased DNMT3a in DRG at the early phase also participate in the paclitaxel-induced downregulation of DRG $K_{2p}1.1$ at the late phase. This possibility remains to be further confirmed.

The paclitaxel-induced downregulation of DRG $K_{2p}1.1$ may be required for paclitaxel-induced pain hypersensitivity. As $K_{2p}1.1$ is opened at rest and capable of driving the membrane potential towards the equilibrium potentials for K^+ [42, 43], it controls neuronal excitability by setting the resting membrane potential and input resistance [43, 44]. We reported that mimicking the paclitaxel-induced downregulation of DRG $K_{2p}1.1$ not only decreased the $K_{2p}1.1$-associated outward potassium current, but also depolarized the resting membrane potential, reduced the current threshold for action potential generation and increased the number of action potentials in small, medium, and large DRG neurons. These findings suggest that the paclitaxel-induced downregulation of DRG $K_{2p}1.1$ may elevate DRG neuronal excitability. The latter likely drives the persistent release of neurotransmitters from the primary afferent terminals, resulting in spinal central sensitization and pain hypersensitivities under the CIPNP conditions. This conclusion was supported by our

behavioral observations that rescuing the paclitaxel-induced downregulation of DRG $K_{2p}1.1$ attenuated the paclitaxel-induced mechanical allodynia and heat hyperalgesia during the development and maintenance periods. Thus, DNMT3a-triggered downregulation of DRG $K_{2p}1.1$ may play a critical role in the CIPNP.

In conclusion, the present study demonstrated a DNMT3a-triggered epigenetic mechanism of DRG $K_{2p}1.1$ downregulation after systemic administration of paclitaxel. Given that rescuing this downregulation impaired the paclitaxel-induced pain hypersensitivity without affecting acute pain and locomotor function, DRG $K_{2p}1.1$ may be a potential target for the management of the CIPNP.

Supplementary Material

Refer to Web version on PubMed Central for supplementary material.

Acknowledgements

We thank Dr. Maha Abdellatif (Rutgers New Jersey Medical School, Newark, NJ) for viral plasmid vector. This work was supported by NIH grants (DA033390, NS094664, NS094224 and HL117684) and Young Scientists Fund of the National Natural Science Foundation of China (Grant No. 81701116).

References

1. Grisold W, Cavaletti G, Windebank AJ. Peripheral neuropathies from chemotherapeutics and targeted agents: diagnosis, treatment, and prevention. Neuro Oncol 2012;14 Suppl 4:iv45–iv54. [PubMed: 23095830]
2. Windebank AJ, Grisold W. Chemotherapy-induced neuropathy. J Peripher Nerv Syst 2008;13:27–46. [PubMed: 18346229]
3. Boyette-Davis JA, Cata JP, Zhang H, Driver LC, Wendelschafer-Crabb G, Kennedy WR, et al. Follow-up psychophysical studies in bortezomib-related chemoneuropathy patients. J Pain 2011;12:1017–24. [PubMed: 21703938]
4. Cata JP, Weng HR, Burton AW, Villareal H, Giralt S, Dougherty PM. Quantitative sensory findings in patients with bortezomib-induced pain. J Pain 2007;8:296–306. [PubMed: 17175202]
5. Argyriou AA, Bruna J, Marmiroli P, Cavaletti G. Chemotherapy-induced peripheral neurotoxicity (CIPN): an update. Crit Rev Oncol Hematol 2012;82:51–77. [PubMed: 21908200]
6. Grisold W, Cavaletti G, Windebank AJ. Peripheral neuropathies from chemotherapeutics and targeted agents: diagnosis, treatment, and prevention. Neuro Oncol 2012;14 Suppl 4:iv45–iv54. [PubMed: 23095830]
7. Alberts DS, Noel JK. Cisplatin-associated neurotoxicity: can it be prevented? Anticancer Drugs 1995;6:369–83. [PubMed: 7670134]
8. Casey EB, Jellife AM, Le Quesne PM, Millett YL. Vincristine neuropathy. Clinical and electrophysiological observations. Brain 1973;96:69–86. [PubMed: 4348690]
9. Devor M Unexplained peculiarities of the dorsal root ganglion. Pain 1999;Suppl 6:S27–S35. [PubMed: 10491970]
10. Jimenez-Andrade JM, Herrera MB, Ghilardi JR, Vardanyan M, Melemedjian OK, Mantyh PW. Vascularization of the dorsal root ganglia and peripheral nerve of the mouse: implications for chemical-induced peripheral sensory neuropathies. Mol Pain 2008;4:10. [PubMed: 18353190]
11. Zhang H, Dougherty PM. Enhanced excitability of primary sensory neurons and altered gene expression of neuronal ion channels in dorsal root ganglion in paclitaxel-induced peripheral neuropathy. Anesthesiology 2014;120:1463–75. [PubMed: 24534904]

12. Sisignano M, Angioni C, Park CK, Meyer Dos SS, Jordan H, Kuzikov M, et al. Targeting CYP2J to reduce paclitaxel-induced peripheral neuropathic pain. Proc Natl Acad Sci U S A 2016;113:12544–9. [PubMed: 27791151]
13. Li Y, North RY, Rhines LD, Tatsui CE, Rao G, Edwards DD, et al. DRG Voltage-Gated Sodium Channel 1.7 Is Upregulated in Paclitaxel-Induced Neuropathy in Rats and in Humans with Neuropathic Pain. J Neurosci 2018;38:1124–36. [PubMed: 29255002]
14. Li Y, Tatsui CE, Rhines LD, North RY, Harrison DS, Cassidy RM, et al. Dorsal root ganglion neurons become hyperexcitable and increase expression of voltage-gated T-type calcium channels (Cav3.2) in paclitaxel-induced peripheral neuropathy. Pain 2017;158:417–29. [PubMed: 27902567]
15. Li Y, Zhang H, Zhang H, Kosturakis AK, Jawad AB, Dougherty PM. Toll-like receptor 4 signaling contributes to Paclitaxel-induced peripheral neuropathy. J Pain 2014;15:712–25. [PubMed: 24755282]
16. Zhang H, Boyette-Davis JA, Kosturakis AK, Li Y, Yoon SY, Walters ET, et al. Induction of monocyte chemoattractant protein-1 (MCP-1) and its receptor CCR2 in primary sensory neurons contributes to paclitaxel-induced peripheral neuropathy. J Pain 2013;14:1031–44. [PubMed: 23726937]
17. Yilmaz E, Gold MS. Sensory neuron subpopulation-specific dysregulation of intracellular calcium in a rat model of chemotherapy-induced peripheral neuropathy. Neuroscience 2015;300:210–8. [PubMed: 25982563]
18. Ito N, Sakai A, Miyake N, Maruyama M, Iwasaki H, Miyake K, et al. miR-15b mediates oxaliplatin-induced chronic neuropathic pain through BACE1 down-regulation. Br J Pharmacol 2017;174:386–95. [PubMed: 28012171]
19. Makker PG, Duffy SS, Lees JG, Perera CJ, Tonkin RS, Butovsky O, et al. Characterisation of Immune and Neuroinflammatory Changes Associated with Chemotherapy-Induced Peripheral Neuropathy. PLoS One 2017;12:e0170814. [PubMed: 28125674]
20. Nie B, Liu C, Bai X, Chen X, Wu S, Zhang S, et al. AKAP150 involved in paclitaxel-induced neuropathic pain via inhibiting CN/NFAT2 pathway and downregulating IL-4. Brain Behav Immun 2018;68:158–68. [PubMed: 29056557]
21. Kindler CH, Yost CS. Two-pore domain potassium channels: new sites of local anesthetic action and toxicity. Reg Anesth Pain Med 2005;30:260–74. [PubMed: 15898030]
22. Mao Q, Yuan J, Ming X, Wu S, Chen L, Bekker A, et al. Role of dorsal root ganglion K2p1.1 in peripheral nerve injury-induced neuropathic pain. Mol Pain 2017;13:1744806917701135.
23. Pollema-Mays SL, Centeno MV, Ashford CJ, Apkarian AV, Martina M. Expression of background potassium channels in rat DRG is cell-specific and down-regulated in a neuropathic pain model. Mol Cell Neurosci 2013;57:1–9. [PubMed: 23994814]
24. Sun L, Zhao JY, Gu X, Liang L, Wu S, Mo K, et al. Nerve injury-induced epigenetic silencing of opioid receptors controlled by DNMT3a in primary afferent neurons. Pain 2017;158:1153–65. [PubMed: 28267064]
25. Zhao JY, Liang L, Gu X, Li Z, Wu S, Sun L, et al. DNA methyltransferase DNMT3a contributes to neuropathic pain by repressing Kcna2 in primary afferent neurons. Nat Commun 2017;8:14712. [PubMed: 28270689]
26. Xu B, Cao J, Zhang J, Jia S, Wu S, Mo K, et al. Role of MicroRNA-143 in Nerve Injury-Induced Upregulation of Dnmt3a Expression in Primary Sensory Neurons. Front Mol Neurosci 2017;10:350. [PubMed: 29170626]
27. Xu JT, Zhou X, Zhao X, Ligons D, Tiwari V, Lee CY, et al. Opioid receptor-triggered spinal mTORC1 activation contributes to morphine tolerance and hyperalgesia. J Clin Invest 2014;124:592–603. [PubMed: 24382350]
28. Zhang J, Liang L, Miao X, Wu S, Cao J, Tao B, et al. Contribution of the Suppressor of Variegation 3–9 Homolog 1 in Dorsal Root Ganglia and Spinal Cord Dorsal Horn to Nerve Injury-induced Nociceptive Hypersensitivity. Anesthesiology 2016;125:765–78. [PubMed: 27483126]
29. Deng L, Guindon J, Cornett BL, Makriyannis A, Mackie K, Hohmann AG. Chronic cannabinoid receptor 2 activation reverses paclitaxel neuropathy without tolerance or cannabinoid receptor 1-dependent withdrawal. Biol Psychiatry 2015;77:475–87. [PubMed: 24853387]

30. Liang L, Gu X, Zhao JY, Wu S, Miao X, Xiao J, et al. G9a participates in nerve injury-induced Kcna2 downregulation in primary sensory neurons. Sci Rep 2016;6:37704. [PubMed: 27874088]
31. Liang L, Zhao JY, Gu X, Wu S, Mo K, Xiong M, et al. G9a inhibits CREB-triggered expression of mu opioid receptor in primary sensory neurons following peripheral nerve injury. Mol Pain 2016;12:1–16.
32. Monsey MS, Ota KT, Akingbade IF, Hong ES, Schafe GE. Epigenetic alterations are critical for fear memory consolidation and synaptic plasticity in the lateral amygdala. PLoS One 2011;6:e19958. [PubMed: 21625500]
33. Brebi-Mieville P, Ili-Gangas C, Leal-Rojas P, Noordhuis MG, Soudry E, Perez J, et al. Clinical and public health research using methylated DNA immunoprecipitation (MeDIP): a comparison of commercially available kits to examine differential DNA methylation across the genome. Epigenetics 2012;7:106–12. [PubMed: 22207357]
34. Nieto FR, Entrena JM, Cendan CM, Pozo ED, Vela JM, Baeyens JM. Tetrodotoxin inhibits the development and expression of neuropathic pain induced by paclitaxel in mice. Pain 2008;137:520–31. [PubMed: 18037242]
35. Liang L, Lutz BM, Bekker A, Tao YX. Epigenetic regulation of chronic pain. Epigenomics 2015;7:235–45. [PubMed: 25942533]
36. LaPlant Q, Vialou V, Covington HE III, Dumitriu D, Feng J, Warren BL, et al. Dnmt3a regulates emotional behavior and spine plasticity in the nucleus accumbens. Nat Neurosci 2010;13:1137–43. [PubMed: 20729844]
37. Marsh B, Acosta C, Djouhri L, Lawson SN. Leak K(+) channel mRNAs in dorsal root ganglia: relation to inflammation and spontaneous pain behaviour. Mol Cell Neurosci 2012;49:375–86. [PubMed: 22273507]
38. Pollema-Mays SL, Centeno MV, Apkarian AV, Martina M. Expression of DNA methyltransferases in adult dorsal root ganglia is cell-type specific and up regulated in a rodent model of neuropathic pain. Front Cell Neurosci 2014;8:217. [PubMed: 25152711]
39. Tulleuda A, Cokic B, Callejo G, Saiani B, Serra J, Gasull X. TRESK channel contribution to nociceptive sensory neurons excitability: modulation by nerve injury. Mol Pain 2011;7:30. [PubMed: 21527011]
40. Poetsch AR, Plass C. Transcriptional regulation by DNA methylation. Cancer Treat Rev 2011;37 Suppl 1:S8–12. [PubMed: 21601364]
41. Turek-Plewa J, Jagodzinski PP. The role of mammalian DNA methyltransferases in the regulation of gene expression. Cell Mol Biol Lett 2005;10:631–47. [PubMed: 16341272]
42. Lesage F, Guillemare E, Fink M, Duprat F, Lazdunski M, Romey G, et al. A pH-sensitive yeast outward rectifier K+ channel with two pore domains and novel gating properties. J Biol Chem 1996;271:4183–7. [PubMed: 8626760]
43. Lesage F, Lazdunski M. Molecular and functional properties of two-pore-domain potassium channels. Am J Physiol Renal Physiol 2000;279:F793–F801. [PubMed: 11053038]
44. Talley EM, Lei Q, Sirois JE, Bayliss DA. TASK-1, a two-pore domain K+ channel, is modulated by multiple neurotransmitters in motoneurons. Neuron 2000;25:399–410. [PubMed: 10719894]

Novelty & Impact Statements

Chemotherapy-induced peripheral neuropathic pain (CIPNP) can limit the dosage and selection of anti-cancer drugs, even lead to discontinuation of chemotherapy. DNMT3a-triggered epigenetic mechanism of DRG K2p1.1 downregulation after systemic administration of paclitaxel may be crucial in the development of CIPNP. Our findings may provide a new avenue for the management of chemotherapy induced pain.

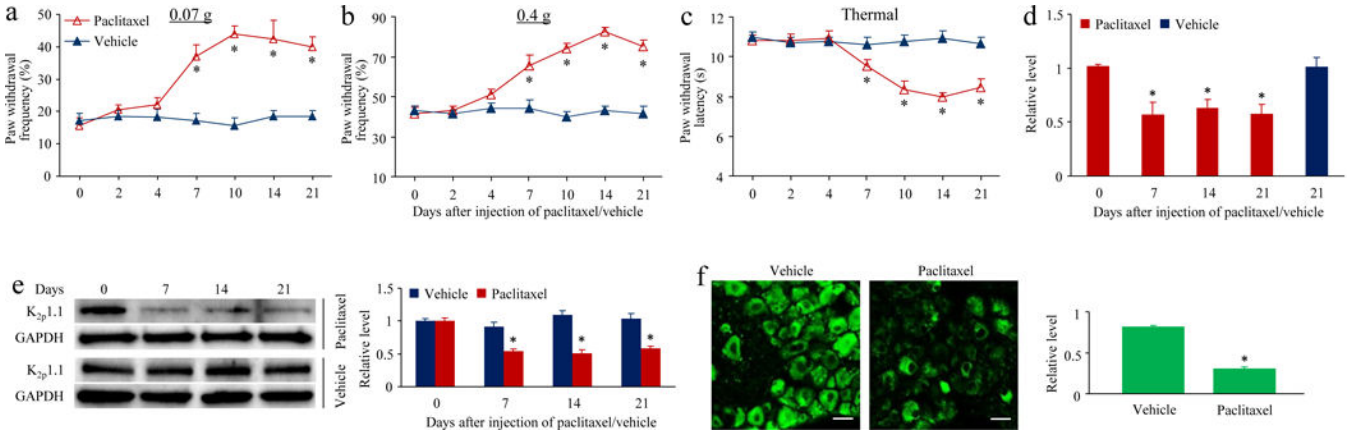

Fig. 1.

Systemic injection of paclitaxel leads to pain hypersensitivities and downregulation of $K_{2p}1.1$ in DRG. (a-c) On the left side, paw withdrawal responses to 0.07 g von Frey filament (a), 0.4 g von Frey filament (b) and heat stimulation (c). n = 12 mice/time point. *$P < 0.05$ *vs* the vehicle-treated group at the corresponding time points by two-way ANOVA followed by post hoc Tukey test. (d) *$K_{2p}1.1$* mRNA expression in L3/4 DRGs on days after first injection of paclitaxel or vehicle. n = 4 biological replicates (8 mice)/time point. *$P < 0.05$ *vs* the corresponding control group (0 day), one-way ANOVA followed by post hoc Tukey test. (e) $K_{2p}1.1$ protein expression in L3/4 DRGs on days after first injection of paclitaxel or vehicle. Representative Western blots (left panels) and a summary of densitometric analysis (right graphs). n = 4 biological replicates (8 mice)/time point. *$P < 0.05$ *vs* the corresponding control group (0 day), two-way ANOVA followed by post hoc Tukey test. (f) Number of $K_{2p}1.1$-labeled neurons in L3/4 DRGs on day 14 after first injection of paclitaxel or vehicle. Representative immunohistochemical staining (left panels) and a summary of the analysis on the number of $K_{2p}1.1$-labeled neurons (right graphs). n = 5 biological replicates (mice)/group. *$P < 0.05$ *vs* the vehicle-treated group by two-tailed paired *t*-test. Scale bar: 20 μm.

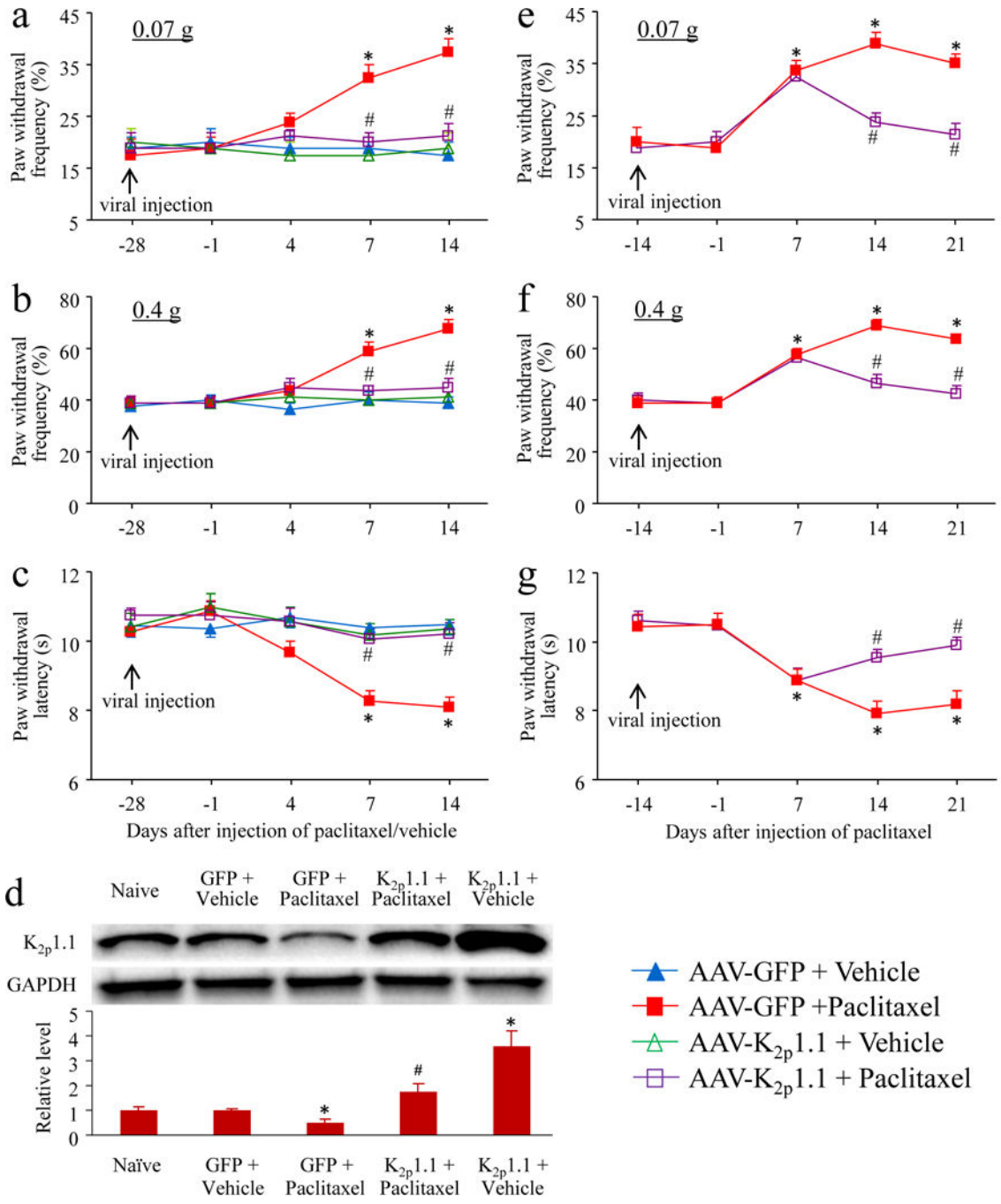

Fig. 2.

Rescuing $K_{2p}1.1$ expression in L3/4 DRGs blocked paclitaxel-induced pain hypersensitivities during the development and maintenance period. GFP: AAV-DJ GFP. $K_{2p}1.1$: AAV-DJ $K_{2p}1.1$. (a-c) Intraperitoneal injection of paclitaxel or vehicle was carried out 4 weeks after microinjection of AAV-$K_{2p}1.1$, or AAV-GFP into the Left L3/4 DRGs. Paw withdrawal responses to 0.07 g von Frey filament (a), 0.4 g von Frey filament (b) and heat stimulation (c) on the ipsilateral (left) side from the treated groups as indicated on days after first injection of paclitaxel or vehicle. n = 12 mice/group. $*P < 0.05$ *vs* the

corresponding baseline (−28 days) by two-way ANOVA followed by post hoc Tukey test. #$P < 0.05$ *vs* the AAV-GFP plus vehicle group at the corresponding time points by two-way ANOVA followed by post hoc Tukey test. (d) $K_{2p}1.1$ protein expression in the ipsilateral (left) L3/4 DRGs on day 14 after first injection of paclitaxel or vehicle in the treated groups as indicated. Representative Western blots (top panels) and a summary of densitometric analysis (bottom graphs). n = 4 biological replicates (8 mice)/group. *$P < 0.05$ *vs* naive mice, # $P < 0.05$ *vs* the AAV-GFP plus paclitaxel group, by one-way ANOVA followed by post hoc Tukey test. (e-g) Intraperitoneal injection of paclitaxel was carried out 2 weeks after microinjection of AAV-$K_{2p}1.1$ or AAV-GFP into the left L3/4 DRGs. Paw withdrawal responses to 0.07 g von Frey filament (e), 0.4 g von Frey filament (f) and heat stimulation (g) on the ipsilateral (left) side from the treated groups as indicated. n = 12 mice/group. *$P < 0.05$ *vs* the baseline (−14 days), or #$P < 0.05$ *vs* the AAV-GFP group at the corresponding time points by two-way ANOVA followed by post hoc Tukey test.

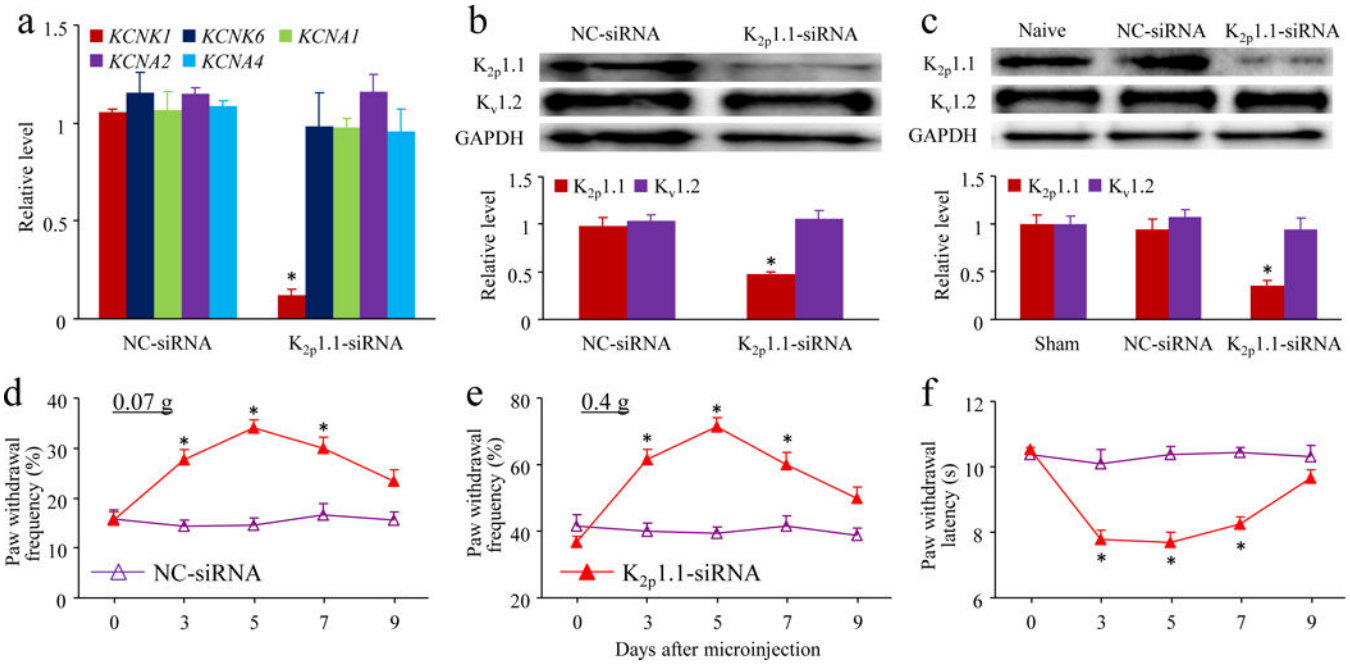

Fig. 3.

DRG $K_{2p}1.1$ knockdown produces neuropathic pain symptoms in mice. NC-siRNA: negative control-siRNA. (a) The levels of *$K_{2p}1.1$, KCNK6, Kcna1, Kcna2, Kcna4* mRNAs in the cultured DRG neurons 3 days after treatment with $K_{2p}1.1$-siRNA or negative control-siRNA. n = 3 repeats per treatment. *$P < 0.05$ *vs* the corresponding NC-siRNA group, by two-tailed paired *t*-test. (b) $K_{2p}1.1$ protein expression in the cultured DRG neurons after treatment with $K_{2p}1.1$-siRNA or negative control-siRNA. n = 5 repeats per treatment. *$P < 0.05$ *vs* the corresponding NC-siRNA group, by two-tailed paired *t*-test. (c) $K_{2p}1.1$ and $K_v1.2$ protein expression in the ipsilateral (Left) L3/4 DRGs 5 days after microinjection of $K_{2p}1.1$-siRNA or negative control-siRNA into these DRGs. n = 4 biological replicates (8 mice)/group. *$P < 0.05$ *vs* naive mice, by one-way ANOVA followed by post hoc Tukey test. (d-f) Paw withdrawal responses to 0.07 g von Frey filament (d), 0.4 g von Frey filament (e) and heat stimulation (f) on the ipsilateral (left) side on days as indicated after microinjection of $K_{2p}1.1$-siRNA or negative control-siRNA into the left L3/4 DRGs. n = 12 mice/time point. *$P < 0.05$ *vs* the NC-siRNA group at the corresponding time points, by two-way ANOVA followed by post hoc Tukey test.

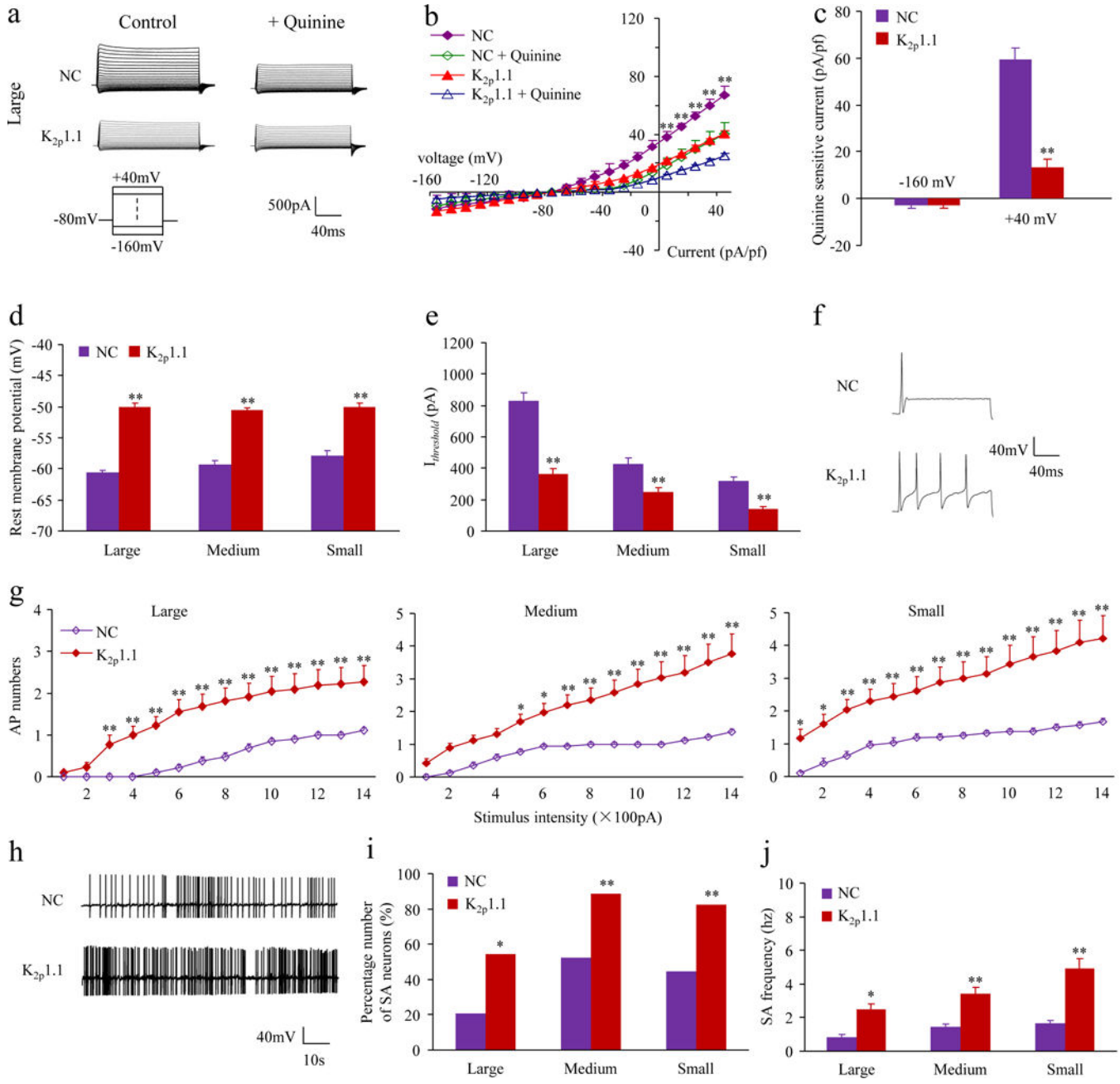

Fig. 4.

$K_{2p}1.1$ knockdown reduces outward potassium channel current and increases the excitability of DRG neurons. NC: negative control-siRNA. $K_{2p}1.1$: $K_{2p}1.1$-siRNA. (a) Representative traces of outward potassium currents in large DRG neurons from the negative control-siRNA-treated and $K_{2p}1.1$-siRNA-treated groups before or after 0.5 mM quinine application. (b) I-V curve for the negative control-siRNA-treated and $K_{2p}1.1$-siRNA-treated groups. n = 19 large neurons from the negative control-siRNA group, n = 22 large neurons from the $K_{2p}1.1$-siRNA group, $^{**}P < 0.01$ *vs* the $K_{2p}1.1$-siRNA group at the corresponding currents, by two-way ANOVA followed by post hoc Tukey test. (c) Quinine sensitive current obtained from current subtraction in large DRG neurons, $^{**}P < 0.01$ *vs* the negative control-siRNA

group by unpaired student's *t*-test. (d-e) Resting membrane potential (d) and current threshold for pulses ($I_{threshold}$, e). n = 22 large, 26 medium and 23 small neurons from negative control-siRNA group (7 mice). n = 24 large, 23 medium and 27 small neurons from the K_{2p}1.1-siRNA group (6 mice). $^{**}P < 0.01$ *vs* the corresponding negative control-siRNA group by two-tailed unpaired Student's *t*-test. (f) Representative traces of the evoked action potentials in DRG neurons. (g) Numbers of the evoked action potentials from the negative control-siRNA-treated and K2p1.1-siRNA-treated groups after application of different currents as indicated. Numbers of the recorded cells are the same as in (d-e). Two-way ANOVA followed by post hoc Tukey test, $^{*}P < 0.05$ or $^{**}P < 0.01$ *vs* the negative control-siRNA-treated group at the corresponding stimulus intensities. (h) Representative traces of spontaneous activity in DRG neurons. (i) Percentage numbers of spontaneous activity (SA) neurons in total recording large, medium and small DRG neurons. $^{*}P < 0.05$ or $^{**}P < 0.01$ *vs* the corresponding negative control-siRNA-treated group by chi-square test. (j) Frequency of spontaneous activity (SA) in DRG neurons. Numbers of the recorded cells are the same as in (a-b). $^{*}P < 0.05$ or $^{**}P < 0.01$ *vs* the negative control-siRNA-treated group by unpaired Student's *t*-test.

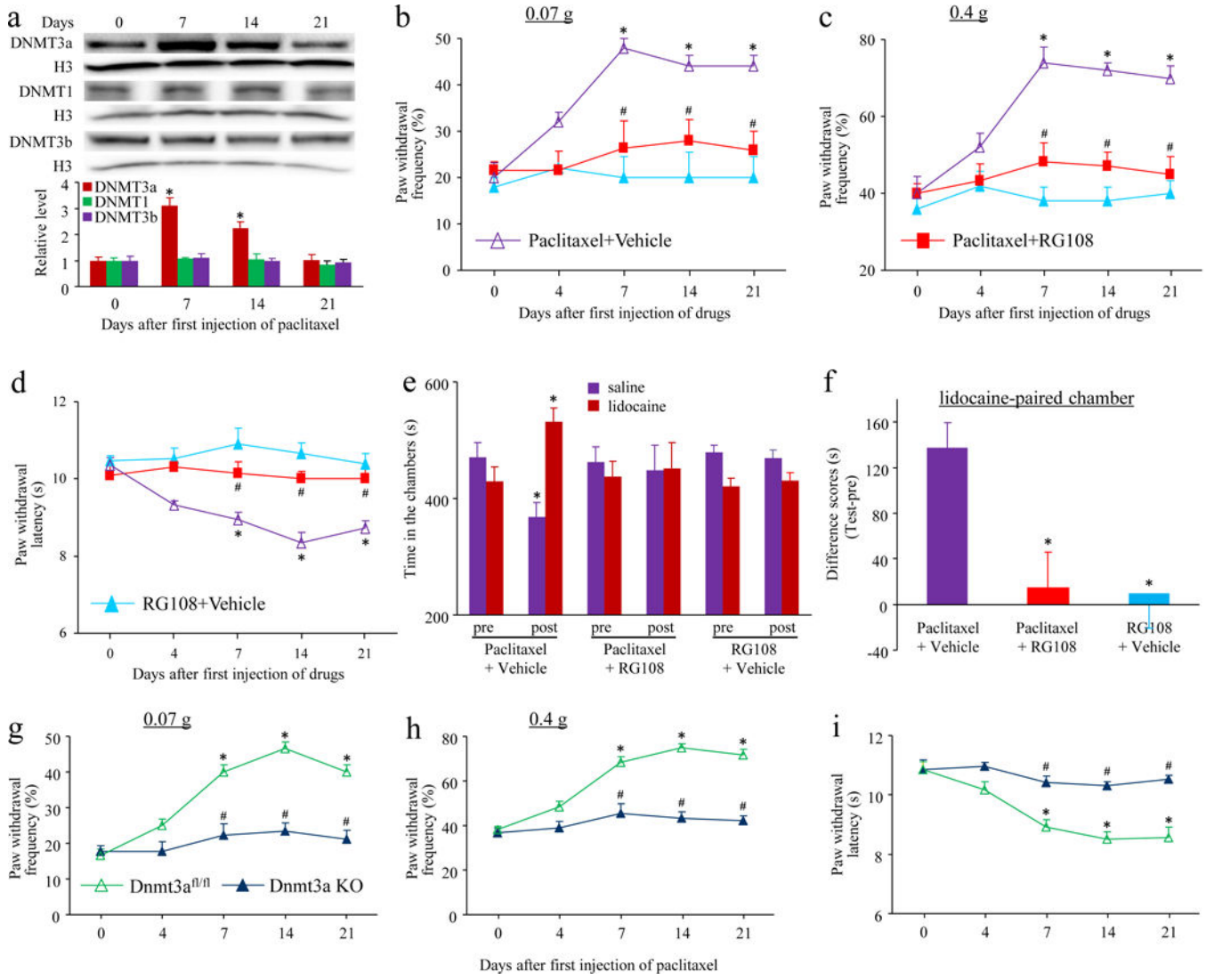

Fig. 5.

Inhibition of DRG DNMT3a activity attenuates paclitaxel-induced neuropathic pain development. (a) Levels of DNMT3a, DNMT1 and DNMT3b in the L3/4 DRGs after first injection of paclitaxel. n = 4 biological replicates (8 mice)/time point. One-way ANOVA followed by post hoc Tukey test. $*P < 0.05$ *vs* the corresponding control group (day 0). (b-d) Effects of co-intraperitoneal injection of RG108 on paw withdrawal responses to 0.07 g von Frey filament (b), 0.4 g von Frey filament (c) and heat stimulation (d) on days as indicated after first intraperitoneal injection of paclitaxel or vehicle. n = 12 mice/time point. $*P < 0.05$ *vs* the baseline (day 0) or $^{\#}P < 0.05$ *vs* the paclitaxel plus vehicle group at the corresponding time points, by two-way ANOVA followed by post hoc Tukey test. (e, f) Effects of co-intraperitoneal injection of RG108 on paclitaxel-induced spontaneous ongoing pain by adopting conditional place preference paradigm. n = 12 mice/group. $*P < 0.05$ *vs* the corresponding preconditioning by two-way ANOVA followed by post hoc Tukey test (e) or the paclitaxel plus vehicle group by one-way ANOVA followed by post hoc Tukey test (f). (g–i) Paw withdrawal responses to 0.07 g von Frey filament (g), 0.4 g von Frey filament (h)

and heat stimulation (i) on the left side of DNMT3a KO mice or DNMT3a$^{fl/fl}$ mice. n = 12 mice/time point. $^{*}P < 0.05$ *vs* the baseline (day 0), $^{\#}P < 0.05$ *vs* the control group (DNMT3a$^{fl/fl}$ mice) at the corresponding time points by two-way ANOVA followed by post hoc Tukey test.

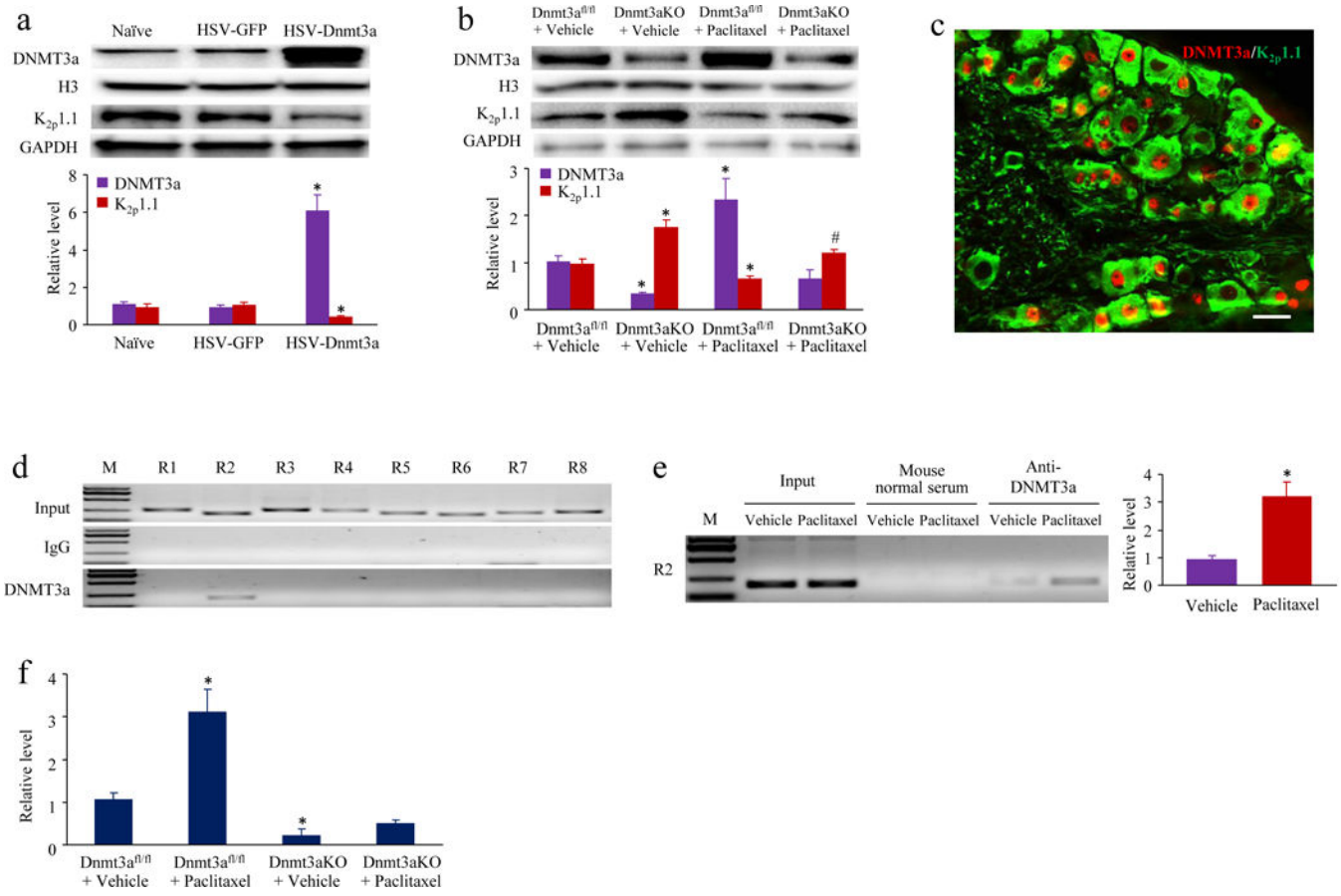

Fig. 6.

DNMT3a regulates the expression of $K_{2p}1.1$ in the DRG neurons. (a) $K_{2p}1.1$ and DNMT3a protein expression in the ipsilateral (left) L3/4 DRGs after microinjection of HSV-Dnmt3a or HSV-GFP into the left L3/4 DRGs. n = 4 biological replicates (8 mice)/group. $*P < 0.05$ *vs* the corresponding naive group, by one-way ANOVA followed by post hoc Tukey test. (b) DNMT3a and $K_{2p}1.1$ protein expression in the L3/4 DRGs from DNMT3a KO mice or control DNMT3a$^{fl/fl}$ mice on day 7 after first injection of paclitaxel or vehicle. n = 4 biological replicates (8 mice)/group. $*P < 0.05$ *vs* the vehicle-treated from the DNMT3a$^{fl/fl}$ mice, by one-way ANOVA followed by post hoc Tukey test. (c) Neurons double labelled by $K_{2p}1.1$ and DNMT3a in the L3/4 DRGs from naive mice. n = 5 mice/group. Scale bar: 40 μm. (d) One region (R2, −596/−406), but not other regions (R1, −791/−541; R3, −424/−175; R4, −192/+47; R5, −17/+168; R6, +148/+323; R7, +269/+470; R8, +448/+661), of the *$K_{2p}1.1$* gene promoter was immunoprecipitated by anti-DNMT3a in the L3/4 DRGs from naive mice. Input: total purified fragments. M: ladder marker. n = 8 repeats. (e) DNMT3a binding to region 2 (R2) of the *$K_{2p}1.1$* gene promoter in L3/4 DRGs on day 14 after first injection of paclitaxel or vehicle. Left: representative binding of Dnmt3a to region 2. Right: the quantitative analysis of the binding. n = 3 biological repeats (8 mice/repeat/group). $*P <$ 0.05 *vs* the vehicle-treated group by two-tailed unpaired Student's *t*-test. (f) DNA methylation levels in region 2 (R2) of the *$K_{2p}1.1$* gene promoter in L3/4 DRGs from the Dnmt3a KO mice or Dnmt3a$^{fl/fl}$ mice on day 14 after first injection of paclitaxel or vehicle.

n = 3 biological repeats (8 mice/repeat/group). *$P < 0.05$ *vs* the vehicle-treated group from the DNMT3a$^{fl/fl}$ mice, by one-way ANOVA followed by post hoc Tukey test.